Laser and Particle Beams (2008), *26*, 619–635. Printed in the USA.

doi:10.1017/S0263034608000694

Fore-vacuum plasma-cathode electron sources

V.A. BURDOVITSIN AND E.M. OKS
Tomsk State University of Control Systems and Radioelectronics, Tomsk, Russia
(RECEIVED 7 April 2008; ACCEPTED 6 October 2008)

Abstract

This paper presents a review of physical principles, design, and performances of plasma-cathode direct current (dc) electron beam guns operated in so called fore-vacuum pressure (1–15 Pa). That operation pressure range was not reached before for any kind of electron sources. A number of unique parameters of the e-beam were obtained, such as electron energy (up to 25 kV), dc beam current (up 0.5 A), and total beam power (up to 7 kW). For electron beam generation at these relatively high pressures, the following special features are important: high probability of electrical breakdown within the accelerating gap, a strong influence of back-streaming ions on both the emission electrode and the emitting plasma, generation of secondary plasma in the beam propagation region, and intense beam-plasma interactions that lead in turn to broadening of the beam energy spectrum and beam defocusing. Yet other unique peculiarities can occur for the case of ribbon electron beams, having to do with local maxima in the lateral beam current density distribution. The construction details of several plasma-cathode electron sources and some specific applications are also presented.

Keywords: E-gun; Fore-vacuum pressure range; Hollow cathode discharge; Plasma-cathode electron source; Ribbon electron beam

1. INTRODUCTION

Though electron beams are today often generated by intense laser interaction with matter (Koyama *et al.*, 2006; Lifschitz *et al.*, 2006; Mangles *et al.*, 2006; Nakamura *et al.*, 2006; Niu *et al.*, 2008; Sakai *et al.*, 2006), the research field of a beam generation by gas discharges and acceleration by pulsed power technique is still of great interest from the view point of scientists and engineers (Dewald *et al.*, 1998; Frank *et al.*, 1998, 1999; Liu, Yin *et al.,* 2007; Liu, Zhan *et al.,* 2007; Wong *et al.*, 2007). A plasma-cathode electron source is an electron beam generator in which the beam is formed by electron emission from a plasma surface. Traditional plasma-cathode electron sources use steady-state or quasi-steady-state plasma discharge systems with discharge current pulse length much greater than the time required for the discharge to reach steady state. In plasma electron sources of this type, as a rule, the discharge system contains no thermionic (hot) cathode, and electrons are emitted from the stabilized plasma boundary. Plasma electron sources produce greater emission current density than hot-cathode systems, are capable of pulsed emission, operate over wide range of background gas pressure and are only weakly dependent on the residual vacuum conditions. The physics and application of electron beams produced by plasma-cathode systems have been discussed in detail (Kreindel, 1977; Zaviyalov *et al.*, 1989; Oks, 2006), reviews (Oks, 1992; Oks & Schanin, 1999; Koval *et al.*, 1992; Gushenets *et al.*, 2003; Bugaev *et al.*, 2003), and original papers (Goebel & Watking, 2000; Hershcovitch, 1993; Krasik *et al.*, 2005; Osipov & Rempe, 2000).

The absence of hot electrodes is one of the major advantages of plasma-cathode electron sources over thermal emitters. This feature allows, among other things, e-beam production at relatively high residual gas pressure. Electron beams can be formed by these systems in a substantially higher-pressure range of up to fore-vacuum pressure (1–15 Pa), where the vacuum can be produced using only a single, simple stage of mechanical pumping. As well as their fundamental interest, the production of electron beams at these high pressures is of practical significance, since it greatly extends the capabilities of relevant technologies and opens up new avenues for applications of electron beams. The feasibility of electron beam production in the fore-vacuum pressure range has no alternative, and offers great promise for the development of these sources. Here we review the current state of the art of fore-vacuum pressure plasma-cathode electron sources.

Address correspondence and reprint requests to: Efim Oks, Tomsk State University of Control Systems and Radio-electronics, 40 Lenin Ave., 634050 Tomsk, Russia. E-mail: oks@fet.tusur.ru

2. SOME FEATURES OF DISCHARGES AND ELECTRON BEAMS IN THE FORE-VACUUM PRESSURE RANGE

2.1. General Principles

The generation of electron beams in plasma-cathode systems requires a compromise between two conflicting requirements. To provide the necessary e-beam parameters, high plasma density, and efficient gas ionization within the plasma discharge must be provided. On the other hand, acceleration of electrons to the required energies assumes high electric field strength within the acceleration gap, which is attainable only if conditions precluding gaseous ionization are established in this region. In traditional plasma sources, a pressure difference maintained between the plasma generation region and the electron beam formation region solves this problem. In the fore-vacuum pressure range however, there is little or no possibility for significant pressure differences—the plasma electron source operates in effect in an isobaric mode. For near-equal pressures, a significant difference in the ionization rates can be obtained only with geometrically different electrode systems in the discharge and in the acceleration gap. A good solution is to combine a hollow-cathode discharge chamber and a plane-parallel acceleration system with electrode gap as small as possible (Mytnikov *et al.*, 1998; Burdovitsin & Oks, 1999). Electron oscillations in the hollow cathode provides efficient plasma generation, and the short time needed for electrons to transit the acceleration gap decreases the probability of gas ionization within the gap, thus precluding gap breakdown. Figure 1 shows a simplified schematic of a fore-vacuum pressure hollow-cathode plasma source for a focused electron beam. At first glance, this electrode system is similar to that of traditional lower pressure e-beam sources. The nuances and details that provide stable operation of the plasma source lie in the design of the acceleration system and the emission (plasma) electrodes. These design features are described in the next section.

The hollow-cathode discharge is stable in the fore-vacuum pressure range, and hence the emission plasma is rather easy to produce. A number of concerns arise with electron extraction from the plasma and with beam formation. The first serious concern is the formation of a stable plasma boundary. This problem is solved by using an emission electrode with a grid or a perforated plate to provide so-called "grid stabilization" (Zaviyalov *et al.*, 1989). A necessary condition for grid stabilization is comparability of the near-electrode space-charge layer in the plane of the emission hole and the hole diameter. The second no-less important concern lies in providing high and controllable emission current. This concern is met *via* the simple relation

$$I_e = j_e S_e, \tag{1}$$

where I_e is the emission current, j_e is the emission current density, and S_e is the plasma emission surface area. The

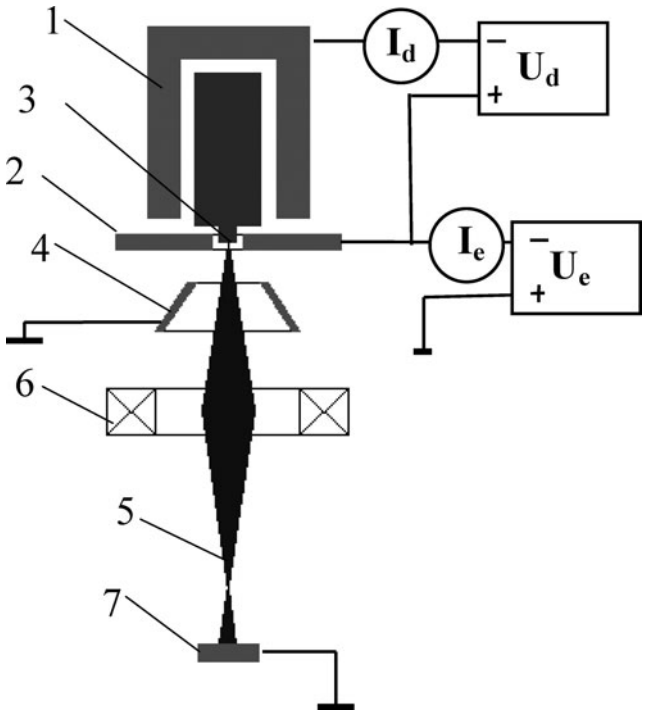

Fig. 1. Electrode system of a fore-vacuum pressure plasma source of focused electron beams: hollow cathode (**1**), anode (**2**), emission hole or channel (**3**), accelerating electrode or extractor (**4**), electron beam (**5**), focusing magnetic lens (**6**), collector (**7**).

values of j_e and S_e are determined by the plasma density and are controllable by varying the discharge current. Finally, a third concern is electron acceleration to the required energy. Clearly, at elevated pressures this is a critical concern since the electric field strength within the gap must be decreased with increasing gas pressure.

The generation of e-beams at elevated gas pressures necessarily leads to greater ionization of residual gas in the electron acceleration and transport regions, and the resulting beam plasma affects the electron beam drift to the collector. However, the backward ion flow ("back-streaming ions") from the drift region to the discharge system of a plasma electron source plays an important part here. The influence of these ions cannot be disregarded when considering the ionization and the formation of the plasma emission boundary, and these ions are, to be sure, significant in determining the electric field of the acceleration gap. The profound effect of back-streaming ions is an essential feature of fore-vacuum pressure plasma-cathode e-beam sources. The backward ion flow modifies the emission properties of traditional plasma-cathode sources operating at lower pressure (Gruzdev *et al.*, 1974). However in the fore-vacuum pressure case, the influence is great.

Another peculiar feature of fore-vacuum plasma e-beam sources is the ignition of a high-voltage glow discharge within the acceleration gap upon application of voltages greater than several kilovolts (Denbnovetsky *et al.*, 2003). Special geometry and specific plasma operation conditions

https://doi.org/10.1017/S0263034608000694 Published online by Cambridge University Press

allow this parasitic discharge to be held to low current. The current of the parasitic high-voltage glow discharge in the acceleration gap is much less than the electron beam current formed by the fore-vacuum pressure plasma source and the voltage distribution across the acceleration gap is unaffected. Thus the high-voltage glow discharge in the acceleration gap has only a marginal effect on the parameters of the source. At the same time, this discharge can be used to ignite the main hollow-cathode discharge.

2.2. Primary Hollow-Cathode Discharge Initiated by Back-Streaming Ions

Despite its relatively low current, the back-streaming ion flux, when penetrating from the region of the high-voltage glow discharge into the discharge chamber of the plasma source, may assist in initiating the primary hollow-cathode discharge. It has been found that application of the acceleration voltage allows the initiating voltage of the main discharge to be reduced, and the dependence of the discharge initiating voltage U_{di} on the acceleration voltage is determined primarily by the operating pressure (Fig. 2).

The high-voltage glow discharge in the acceleration gap of a fore-vacuum pressure plasma-cathode electron source has been investigated for application of the accelerating voltage U_e (Fig. 3). In this work, we measured both the discharge parameters in the acceleration gap and the current I_i in the hollow-cathode. In further experiments, the discharge power supply was connected and the correlation between the ion current I_i penetrating into the cathode cavity and the initiating voltage U_{di} of the main discharge was examined.

Visual observations reveal that upon application of the accelerating voltage, a glow occurs in the acceleration gap, indicative of a high-voltage glow discharge. As expected (Denbnovetsky *et al.*, 2003), the current of the high-voltage glow discharge in the acceleration gap increases with

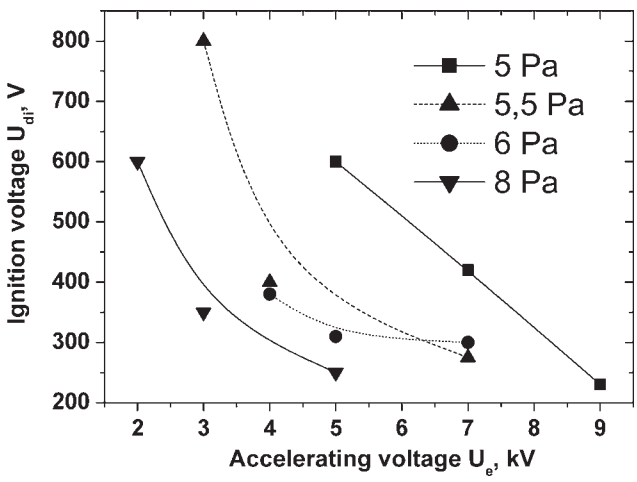

Fig. 2. Discharge ignition voltage U_{di} *versus* voltage U_e across the acceleration gap for different gas pressures.

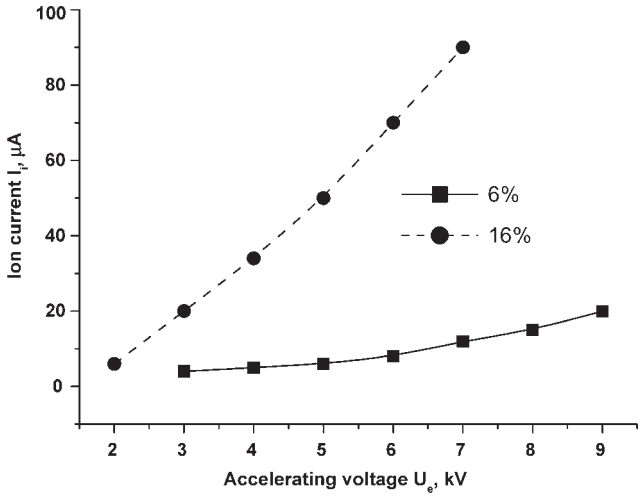

Fig. 3. Ion current I_i in the cathode cavity versus accelerating voltage U_e for different emission electrode transparency. Gas pressure was 4 Pa.

increasing accelerating voltage as well as with gas pressure and gap width. The current I_i in the hollow cathode depends on the accelerating voltage and gas pressure in a similar way (Fig. 3). Apparently this current is governed by the ions accelerated within the high-voltage glow discharge gap and penetrating into the cathode cavity through the emission hole. The experimental evidence for this is the increase in I_i with increasing emission electrode transparency.

The experiments lead to the conclusion that the ignition of the discharge depends largely on the backward ion flow to the cathode cavity, and on the cathode material and the gas species used. For example, replacing a stainless steel cathode by an aluminum cathode decreases the discharge initiating voltage by a factor of 1.5–2. This effect can be estimated using the known expression for the initiation condition of a self-sustained discharge (Raizer, 1991). Taking into account the ions arriving in the cavity from outside, this expression can be written as

$$(\gamma_1 \cdot N_1 + \gamma_2 \cdot N_2)(e^{\alpha d} - 1)/(N_1 + N_2) = 1, \qquad (2)$$

where N_1 is the number of ions in the discharge gap without high-voltage glow discharge, N_2 is the number of ions arriving from the acceleration gap, γ_1 is the ion-electron emission coefficient for ions produced in the discharge gap, γ_2 is the ion-electron emission coefficient for ions penetrating into the discharge gap. The difference between γ_1 and γ_2 is determined only by the difference in ion energies. Estimates show that under experimental conditions the ignition of the hollow-cathode discharge is determined mainly by N_2.

During formation of a strongly focused beam, the decrease in beam area leads to a corresponding decrease in the back-streaming ion flux penetrating into the discharge gap through the hole. Undoubtedly this decrease precludes discharge ignition. For discharge ignition under these conditions, a special design of the emission electrode has been

https://doi.org/10.1017/S0263034608000694 Published online by Cambridge University Press

used. The electrode, along with the central emission aperture, had a number of peripheral, smaller holes surrounding the central hole. The diameter of the peripheral holes was chosen to be sufficiently small that the space charge layers overlapped them and efficient emission was thus reduced. At the same time, the total area of these holes was sufficient to ensure the required flow of discharge-initiating back-streaming ions. The ignition of the main discharge by back-streaming ion flow from the parasitic high-voltage discharge is described at greater length in (Zhirkov *et al.*, 2006*b*).

2.3. Formation of the Plasma Emission Boundary

A plasma cathode is characterized by a moving emission boundary (Kreindel, 1977; Zaviyalov *et al.*, 1989), because this kind of cathode always provides the saturation current. The plasma emission surface is normally stabilized by decreasing the size of the elementary emission hole(s) to a value comparable with the thickness of the ion layer separating the plasma from the emission electrode (Zharinov *et al.*, 1986*a*; Galansky *et al.*, 1987). Failure to fulfill the condition of layer stabilization means that electrons are extracted from a so-called open plasma surface for which the emission characteristics are unstable. This may lead to instability in the emission current and finally to breakdown in the acceleration gap.

One of the fundamental features of plasma cathodes in the fore-vacuum pressure range is a strong effect of the back-streaming ion flow from the acceleration gap and from the electron beam transport region. This effect is responsible for, among other things, partial or complete compensation (or neutralization) of the space charge of beam electrons. This in turn changes the potential distribution within the acceleration gap and affects its transmittance. Another important factor is the increase in emitting plasma density in response to the charge exchange of ions arriving to the plasma. The increase in plasma density inevitably increases the emission current density. At constant accelerating voltage, this may shift the plasma boundary toward the acceleration gap and cause emission from the open plasma surface and breakdown of the acceleration gap.

2.3.1. Effect of the magnetic field on the emission boundary formation

A possible way to guard against instability of the emission current associated with the uncontrollable increase in emission plasma density due to back-streaming ions is to limit the radial plasma expansion by a rather weak (up to 15 mT) axially symmetric longitudinal magnetic field.

The effect of magnetic field has been investigated (Fig. 4). Measurements of the plasma density distribution suggest that the magnetic field reduces radial transport of plasma penetrating into the acceleration gap through the emission hole and confines the plasma to near the system axis. The magnetic field greatly decreases the on-axis plasma potential in

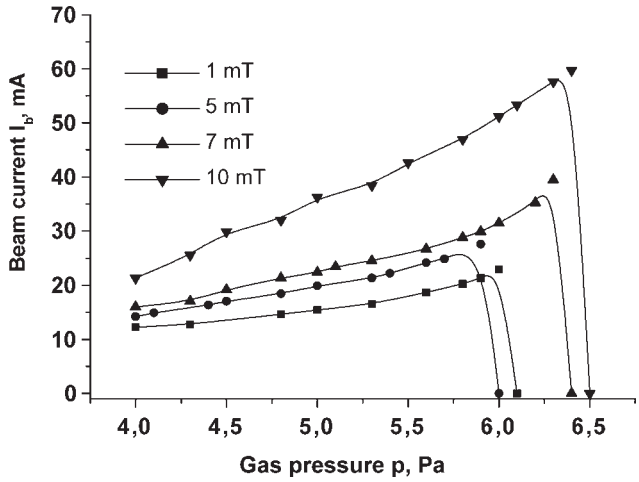

Fig. 4. Electron beam current I_b versus gas pressure p for different magnetic fields. Emission hole diameter $d = 1.2$ mm, accelerating voltage $U_e = 1$ kV, and discharge current is 400 mA.

the immediate vicinity of the anode hole. For low magnetic field, the plasma density increases and saturates. It can be seen in Figure 4 that increasing magnetic field shifts the limiting acceleration gap breakdown pressure toward higher values. The minimum magnetic field precluding the breakdown of the gap increases as the discharge current is increased.

The mechanism of breakdown within the acceleration gap (Burdovitsin *et al.*, 2002) is due to penetration of plasma from the discharge region into the acceleration gap, and subsequent switching of the discharge current from the anode to the accelerating electrode. Limitation of the electric field strength and breakdown of the acceleration gap in a plasma-cathode electron source can be represented in the simplest approximation by applying the known Zharinov *et al.* (1986*b*) relation for a plasma cathode,

$$GS_e/(S_e + S_a) > 1. \quad (3)$$

Here S_e is the plasma emission surface area, S_a is the anode surface area (in the general case, the total area of all electrodes to which electrons from the discharge gap may stream), and G is a discharge parameter approximating the ratio between the chaotic electron current density j_c and the electron current density j to the anode with no electron extraction from the plasma (for discharges with a negative anode potential fall, the parameter G can be far greater then unity, depending on the ionization conditions). From Eq. (3) it follows that the acceleration gap breaks down when the area of the plasma emission surface S_e becomes greater than a certain critical value. Since the radial transport of plasma penetrating into the acceleration gap is limited by the longitudinal magnetic field, we can determine the relationship between the magnetic field, the plasma density, and the plasma boundary area, and hence the switching condition. The physical model used to describe the behavior of

https://doi.org/10.1017/S0263034608000694 Published online by Cambridge University Press

the plasma gives dependences that agree qualitatively with experimental data.

The formation of the plasma emission boundary with regard to the effect of the longitudinal magnetic field in the acceleration gap is described at greater length in Zhirkov *et al.* (2007). The electric field strength of the acceleration gap is considered in Section 2.5.

2.3.2. Features of the formation of an extended plasma emission boundary

In the case of large cross-section electron beams, a specific problem arises with respect to the formation of a uniform plasma boundary. This concern is well known to designers of large-cross-section electron beam sources, particularly ribbon beams (Bugaev *et al.*, 1984). A necessary condition for producing a ribbon beam of uniform cross-sectional current density distribution is the formation of plasma that is uniform in the transverse plane. In the fore-vacuum pressure range, transversely-uniform plasma can be readily formed by an extended hollow cathode discharge for densities in the range $(1–5) \times 10^9$ cm^{-3}. However, attempts to increase the plasma density inevitably result in a nonuniform current density distribution over the beam cross section (Vizir *et al.*, 1997).

Figure 5a shows a simplified schematic of a plasma source for ribbon electron beam generation, designed specially for operation in the fore-vacuum pressure range. The source is comprised of a $310 \times 60 \times 30$ mm^3 rectangular hollow cathode 1, plane anode 2 with a 310×16 mm^2 emission slot-hole, and insulators 3 and 4. The insulators also serve for fixing the electrodes. The height (h) of the cathode cavity is controlled with insert 5. The exit aperture of the cathode cavity is controlled with plates 6 differing in slot-hole widths. The discharge U_d and accelerating U_e voltages are applied to the corresponding electrodes of the source, as shown in the figure. The gas pressure is varied in the range of 3–10 Pa by supplying gas directly to the vacuum chamber to which the electron source is attached.

Measurements show that decreasing the slot-hole width in the cathode cavity aperture increases the plasma density (Fig. 6a). However, with a slot-hole width of 9 mm or less, the plasma distribution along the cavity becomes nonuniform with one or several local peaks, as revealed by the intense glow. The position of these peaks can change abruptly. The most distinct peak is found for small discharge currents. As the discharge current is increased, the peak becomes less visible (Fig. 6b). Decreasing the volume and hence the area of the cathode cavity walls by decreasing the height h (Fig. 5a) decreases the threshold discharge current at which the local peak disappears. The threshold current decreases also with increasing slot-hole width of the cathode cavity aperture and with pressure. The plasma density distribution in the cavity measured by a probe at different immersion depths suggests that the most clearly defined peak is that in the plane of the slit-like aperture.

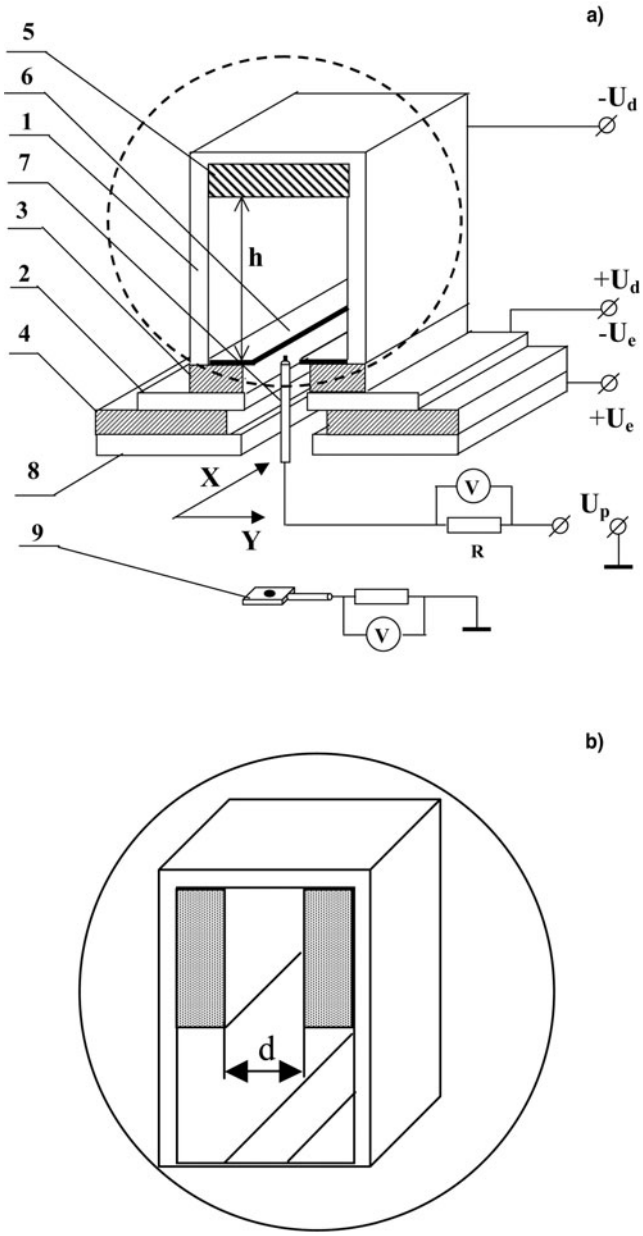

Fig. 5. Plasma source of ribbon electron beam with rectangular (**a**) and cross-sectionally nonuniform (**b**) cathode cavity: hollow cathode (**1**), anode (**2**), insulators (**3**, **4**), insert (**5**), plates (**6**), probe (**7**), accelerating electrode (**8**), and movable collector (**9**).

The experiments show that the slot-hole width is a critical parameter in determining the uniformity of the plasma density distribution. This enables us to propose a plausible mechanism for the phenomenon using the concept of spontaneous "constriction" of the discharge in a local region. At small discharge currents and hence low plasma densities, ion layers overlap the slot-hole in the cathode cavity aperture. A random deviation of plasma density or potential from the steady-state value decreases the ion layer thickness and increases the electron current in this region, resulting in an increase in ionization intensity and in plasma density. This means that the ion layer thickness continues to decrease.

https://doi.org/10.1017/S0263034608000694 Published online by Cambridge University Press

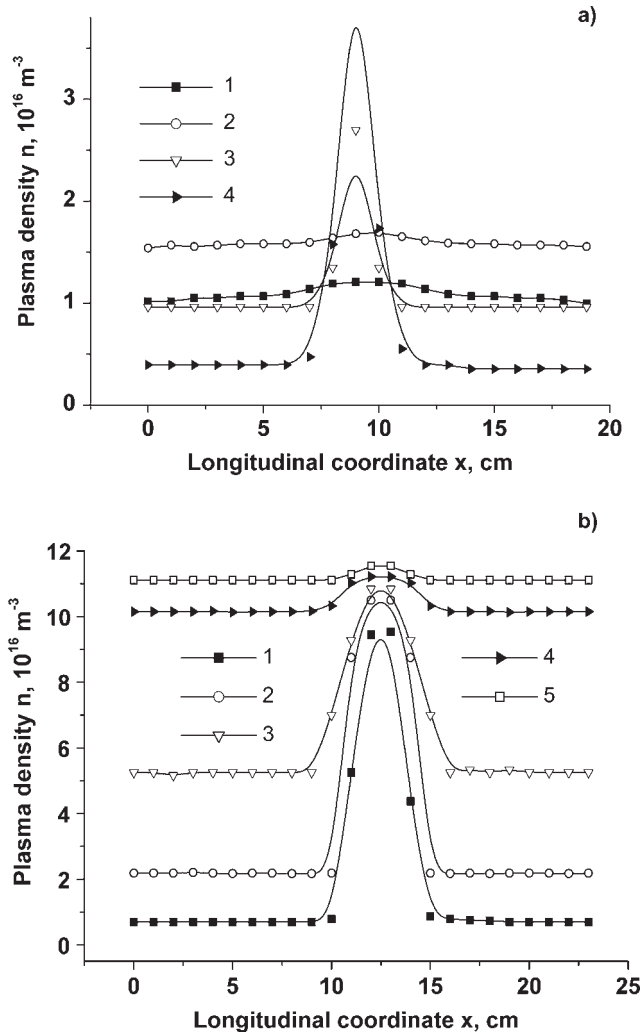

Fig. 6. Plasma density distribution n in the cathode cavity aperture for different slot-hole widths (**a**): 13 (1), 11 (2), 9 (3), and 8 mm (4), for discharge current 400 mA, and for different discharge currents (**b**): 0.2 (1), 0.4 (2), 0.6 (3), 1 (4), and 1.3 A (5), for pressure 6 Pa.

The process develops in an avalanche-like manner and culminates in the formation of a local region through which most of the electron current passes. As the discharge current is increased, the plasma density increases, and the ion sheath beyond the local region is disrupted, changing the character of the plasma density distribution along the cavity length. The foregoing allows us to refine the physical model of the processes used in calculations. The numerical estimates agree satisfactorily with experimental data (Burdovitsin *et al.*, 2004*a*). A more detailed description of research on the formation of extended area plasma emission surfaces in the fore-vacuum pressure range can be found in Burdovitsin *et al.* (2004*b*).

The search for ways to increase the emitting plasma density led to a change in the geometry of the extended cathode cavity (Klimov *et al.*, 2008). Experiments demonstrate that discharges with non-uniform (Fig. 5b) and uniform or rectangular (Fig. 5a) cathode cavity cross sections differ in current-voltage characteristics and plasma parameters. For a cross-sectionally uniform cathode cavity, the discharge current-voltage characteristic is monotonic, whereas for a cross-sectionally non-uniform cathode cavity, an abrupt increase in discharge current and fall in discharge voltage are observed. The plasma density in the symmetry plane of the cavity also increases. The abrupt increase in discharge current and the increase in plasma density result in a brighter plasma glow in the narrow section of the cavity. The threshold value of the current I_d at which the discharge is rearranged is determined by the gas pressure and by the width of the narrow section of the cavity. The lower the pressure and the smaller the width d, the higher the value of I_d. The abrupt jump in the discharge current gives rise to onset of current in the narrow section of the cathode cavity. Moreover, because of the redistribution of the discharge current components, it is within the narrow section that most of the discharge current flows. Ignition of the discharge in the narrow section of the cavity changes drastically the plasma density distribution in the transverse direction y of the cavity (see Fig. 5). The distribution $n(y)$ has a clearly defined maximum of width approximating the width of the narrow section of the cavity (Fig. 7). The maximum density is 1.5–2 times greater than that found for a cross-sectionally uniform cavity at the same discharge current. The higher plasma density is responsible for a corresponding increase in electron beam current density extracted from the plasma (Fig. 8). In our experiments, the current density reached 35 mA/cm^2.

The results can be interpreted in the context of two modes of discharge operation in the cross-sectionally non-uniform cathode cavity. For relatively low current and low plasma density, the discharge operates only in the wide section of the cathode cavity, since the narrow section is overlapped by the cathode layers and the plasma has no way of penetrating into this section. Increasing the discharge current by

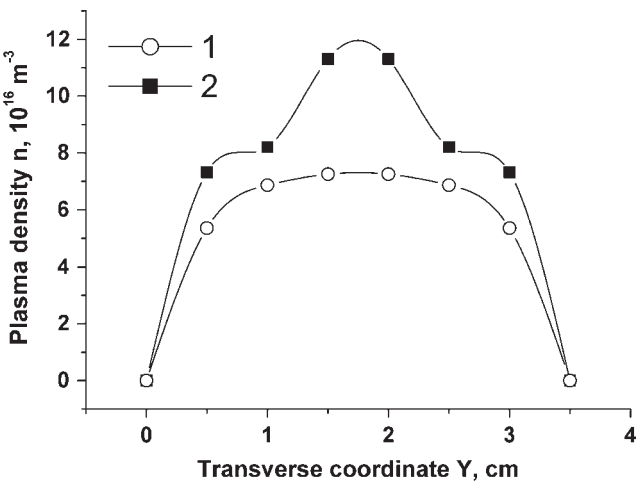

Fig. 7. Transverse plasma density distribution in cross-sectionally uniform (**1**) and nonuniform (**2**) cavity. $I_d = 800$ mA, $d = 16$ mm, $P = 6$ Pa.

https://doi.org/10.1017/S0263034608000694 Published online by Cambridge University Press

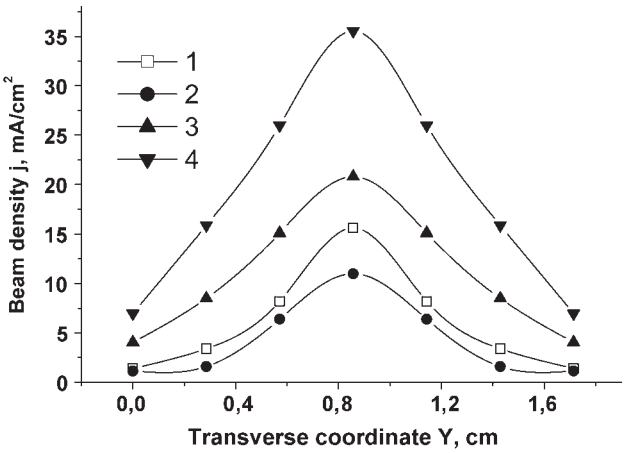

Fig. 8. Current density distribution j in the beam for discharge current $I_d = 100$ mA (1, 2) and 800 mA (3, 4), for rectangular (1, 3) and sectional (2, 4) cavities, $d = 16$ mm, $P = 6$ Pa, $U_e = 2$ kV.

external adjustment makes it possible to reach the point for which the cathode sheath is disrupted and the plasma penetrates into the narrow section of the cavity. The penetration condition is written as (Osipov & Rempe, 2000)

$$d/2 > l_c = (\varepsilon_0/n)^{1/2}(U_c)^{3/4}/(ekT_e)^{1/4}, \quad (4)$$

where d is the width of the narrow section of the cathode cavity, l_c is the thickness of the cathode layer, n and T_e are the plasma density and the electron temperature, respectively, and U_c is the cathode potential fall. Substitution of the measured plasma and discharge parameters in the expression for the threshold current gives $l_c = 0.5$ cm that agrees as a whole with Eq. (4). The abrupt increase in current, along with the decrease in discharge voltage, and the current redistribution between the cavity sections such that most of the current takes the path through the narrow section, unambiguously suggest that the discharge system with a cross-sectionally non-uniform hollow cathode provides conditions for more efficient ionization. The result is somewhat unexpected taking into account that for a cross-sectionally uniform cavity of width equal to the width of the narrow section, attempts to maintain stable operation of the discharge in the operating pressure range have not met with success due to the plasma non-uniformity along the cavity length.

A more detailed description of research on the formation of the extended plasma emission surface in the fore-vacuum pressure range for discharge systems with cross-sectionally uniform and non-uniform cathode cavities can be found elsewhere (Burdovitsin *et al.*, 2004*a*, 2004*b*; Klimov *et al.*, 2008; Burachevsky *et al.*, 2006; Klimov *et al.*, 2007).

2.4. Effect of Back-Streaming Ions on Plasma Emission Properties

The effect of back-streaming ions on the plasma cathode emissivity is an important feature of plasma electron emission in the fore-vacuum pressure range. Back-streaming ions affect the formation of the plasma emission boundary *via* two mechanisms. First, the ion flow is responsible for partial compensation of the negative space charge of electrons, which increases the transmittance of the accelerating gap, and for constant emission current density shifts the plasma boundary away from the accelerating electrode. Second, the back-streaming ions increase the plasma emissivity due to both charge exchange of ions arriving in the plasma and increase in plasma density. For constant gap transmittance, this effect may cause the plasma boundary to move closer to the accelerating electrode. The mechanism dominates depends on the specific conditions.

The influence of back-streaming ions is evidenced by a strong effect of residual gas pressure on the e-gun emissivity. This influence is illustrated by the experimental dependencies shown in Figure 9. It can be seen that increasing the gas pressure for fixed discharge parameters increases the electron emission current. The influence of gas pressure becomes more profound with increasing accelerating voltage.

For the case of large cross-section electron beams, particularly ribbon beams, the effect of back-streaming ions on the plasma emissivity is a greater non-uniformity of the plasma density distribution in the electron extraction region due to positive feedback between the electron emission current and the back-streaming ion current. Experiments show that without electron emission (i.e., without application of accelerating voltage) the plasma non-uniformity along the cavity length is less than 10%. But electron extraction from the plasma at elevated pressures results in much greater non-uniformity in both the plasma and the e-beam. Then the locations of the maxima of the emission current density and the emitting plasma density coincide, and the beam current density distribution has greater non-uniformity than the plasma density distribution. The effect of emission on the current density and plasma density distribution uniformity becomes less pronounced

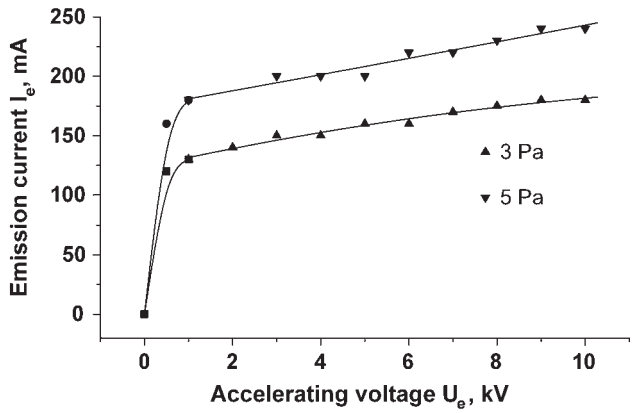

Fig. 9. Emission current I_e versus accelerating voltage U_e for different pressures. $I_d = 0.5$ A, $b = 0.6$ mm, $d = 0.9$ mm.

https://doi.org/10.1017/S0263034608000694 Published online by Cambridge University Press

as the gas pressure and the emission hole (grid mesh) dimensions are decreased.

In the initial phase of electron extraction from the plasma, the current density distribution non-uniformity is determined mainly by the plasma density distribution non-uniformity. The emission grid "non-uniformity" (different local curvatures, and spread in elementary extraction hole size) may also affect the current density distribution. Intense ionization of residual gas in the acceleration gap and in the electron beam transport region gives rise to a large back-streaming ion flux. Because the ionization rate is proportional to the electron current density, the distribution of back-streaming ion current density corresponds to the initial distribution of the electron current density. Energetic ions arriving in the plasma undergo charge exchange with gas molecules, yielding a positive space charge, which is neutralized by plasma electrons. The result is a local increase in the non-uniformity of the plasma density and emission current density distributions. The increase in these parameters is also governed by the increased open plasma surface area within each anode grid mesh aperture due to the decreased thickness of the space charge layer separating the plasma from the grid. Thus a small local change in plasma density causes a disproportional local increase in electron emission current density. The back-streaming ion flux associated with the electron current ensures a further local increase in plasma density and a corresponding disproportional increase in electron emission current in this region. The positive feedback involved eventually saturates, and the plasma density ceases to increase as the production rate of slow ions becomes equal to the rate of their removal from the perturbed region (Burachevsky *et al.*, 2006; Klimov *et al.*, 2007).

2.5. Electric Field Strength in the Acceleration Gap

The main factor limiting the electron beam energy at elevated pressures is insufficient electric field strength in the acceleration gap. In previous work (Burdovitsin *et al.*, 2002; Burachevsky *et al.*, 2001), we have shown that there are two kinds of breakdown within the acceleration gap, differing in their conditions and in parametric relationships. The first type of breakdown, usually called simply an electrode breakdown, occurs between the accelerating electrode and the anode. The second type of breakdown is a plasma breakdown, occurring between the discharge plasma and the accelerating electrode. The type of breakdown that occurs in a particular situation is determined mainly by the size of the emission holes and by the gas pressure within the acceleration gap. Relatively small hole size and low pressure result in an electrode breakdown, whereas large size holes and high pressure result in a plasma breakdown.

In experiments to investigate these features, electrode breakdown was initiated by increasing the voltage across the acceleration gap at fixed emission current. Figure 10 shows the measured gap breakdown voltage U_{em} as a function of electron emission current I_e for different gas pressures. One can see that the breakdown voltage is strongly dependent upon the emission current, and the variation is not monotonic.

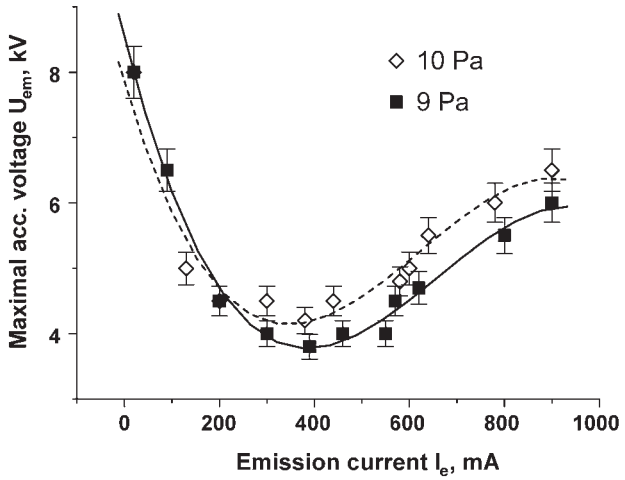

Fig. 10. Limiting accelerating voltage U_{em} *versus* emission current I_e for different pressures.

Note that for an emission current greater than a certain threshold value, an increase in U_{em} is observed. This seemingly unexpected effect was found only for electrode breakdown. Two possible mechanisms for the effect were considered. The first mechanism is local heating of gas during the electron beam transport. Beam electrons ionize gas molecules in inelastic collisions within the acceleration gap, and the resulting ions are accelerated by the electric field and suffer elastic collisions with gas molecules, transferring momentum to them and thus heating the gas. Our estimates show that at an electron current of 1 A, this phenomenon may decrease the neutral gas concentration by a factor of 1.5–2, in turn decreasing the ionization probability. At the same time, we understand that this mechanism is contradictory in a way, and an alternative mechanism, associated with positive ion accumulation in the acceleration gap and thus a non-uniform potential distribution (shortening of the discharge gap), is conceivable. Nevertheless both mechanisms must increase the electric field strength within the acceleration gap, corresponding to the left-hand side of the Paschen curve.

The second type of breakdown (plasma breakdown) was induced experimentally by increasing the discharge current at fixed acceleration gap voltage. Figure 11 shows the measured limiting discharge current I_{dm} as a function of the accelerating voltage U_e. An increase in anode transparency by increasing the number of holes shifts I_{dm} toward higher values. These experiments suggest that in this case it is the discharge current, rather than the emission current, that is responsible for breakdown.

https://doi.org/10.1017/S0263034608000694 Published online by Cambridge University Press

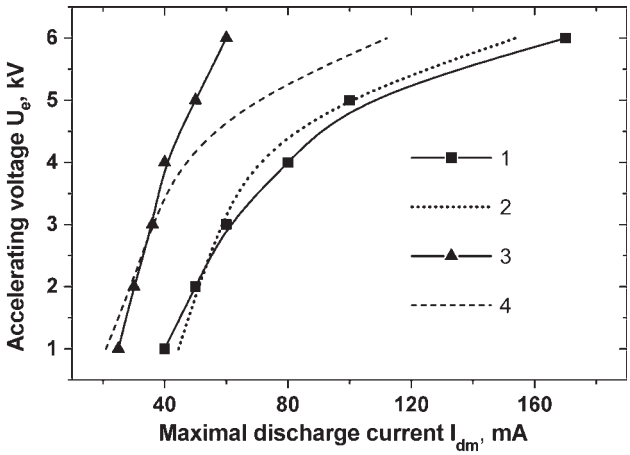

Fig. 11. Limiting discharge current I_{dm} *versus* accelerating voltage U_e for pressures $p = 14$ Pa (1, 2) and $p = 15$ Pa (3, 4), experiment (1, 3), calculation (2, 4).

The difference in the character of the two kinds of breakdown is indicative of their different physical mechanisms. Electrode breakdown should be analyzed taking into account that with no emission, i.e., at $I_d = 0$, application of accelerating voltage results in a high-voltage glow discharge with a current of several mA within the acceleration gap. In the fore-vacuum pressure range, electrical breakdown is properly a transition of discharge from a high-voltage to a low-voltage form. The transition is due to an additional ionizer, which in this case is the electron beam.

The results obtained for the second type of breakdown, i.e., plasma breakdown, can be interpreted using a model described in Burdovitsin *et al.* (2002) and Burachevsky *et al.* (2001). The model assumes that acceleration gap breakdown occurs when plasma from the discharge region penetrates into the gap. There are two conditions for penetration. First, the thickness of the near-anode space-charge layer separating the plasma from the anode must decrease to a value much smaller than the size of the emission holes. Second, the plasma—accelerating gap spacing estimated from the Child–Langmuir law must be less than the length of the acceleration gap. Under these conditions, the discharge current switches from the anode to the accelerating electrode with an abrupt drop in voltage across the acceleration gap, which is what we consider as breakdown. The decrease in near-anode layer thickness is governed mainly by the increase in plasma density in response to both the increase in discharge current and the arrival of gas ions from the acceleration gap. At the same time, the increase in plasma potential (eventually due to increasing accelerating electrode voltage) increases the layer thickness. The plasma potential is taken positive with respect to the anode. This is evidenced by direct measurements with an emission probe. The expression for the plasma potential φ_p can be derived taking into account the current balance and the possibility of the acceleration electrode field penetrating into the emission holes:

$$\varphi_p = \frac{kT_e}{e} \ln\left[\frac{S_a j_c (1 + \xi\left(\exp\left(\frac{eD\varphi_e}{kT_e}\right)\right)}{I_d}\right], \quad (5)$$

where j_c is the plasma electron thermal current density, φ_e is the potential of the accelerating electrode, D is the electrical transparency of the anode, S_a is the anode area, and ξ is the emission-to-anode area ratio.

Using the known expression for the thickness l of the near-anode space-charge layer:

$$l = (\varepsilon_0/n)^{1/2}(\varphi_p - \varphi_a)^{3/4}/(ekT_e)^{1/4}. \quad (6)$$

where φ_a is the anode potential, n is the plasma density, and T_e is the electron temperature, and taking $l = \beta h$ as the condition for plasma penetration from the discharge region into the acceleration gap, we obtain a relationship between the limiting discharge current and the parameters of the discharge-emission system, the gas species, and the pressure:

$$I_{dm} = \frac{4}{(\beta h)^2}\left[\frac{\varepsilon_0 \varphi_p^{3/2}}{\sqrt{ekT_e}}\left(1 - \frac{3}{4} n_n Q_e d_a \frac{Q_i}{Q_n}\sqrt{\frac{MT_e}{mT_i}}\right)\right] \times \left(0.4 \cdot e \cdot S_c \sqrt{\frac{2kT_e}{M}}\right), \quad (7)$$

where n_n is the neutral density in the acceleration gap, Q_e is the cross section for ionization of gas molecules by fast electrons, Q_i is the total interaction cross section of slow ions in the plasma, Q_n is the charge exchange cross section for fast ions, M and T_i are the ion mass and ion temperature in the plasma, d_a is the acceleration gap width, and $\beta < 1$ and is determined experimentally. A calculation using this model agrees satisfactorily with experimental results.

2.6. Processes Involved in Electron Beam Transport

An important feature of e-beam generation and transport at elevated gas pressures is the strong effect of electron interaction with residual gas on the e-beam parameters (Burachevsky *et al.*, 2006). For beam current greater than a certain threshold value, a bright glow is often observed at the focal plane. The spectrum of the glow is rich in lines of low-energy excitation, and the beam energy spectrum is broad (Fig. 12). The beam diameter at the focal plane also increases with beam current. For electron beam current greater than a certain threshold value, an abrupt increase in beam plasma density n and plasma electron temperature T_e is found (Fig. 13). The results shown in Figures 12 and 13 are clearly indicative of collective interactions of the electron beam with the beam-produced plasma (Zhirkov *et al.*, 2006*b*). The minimum e-beam current required for the

https://doi.org/10.1017/S0263034608000694 Published online by Cambridge University Press

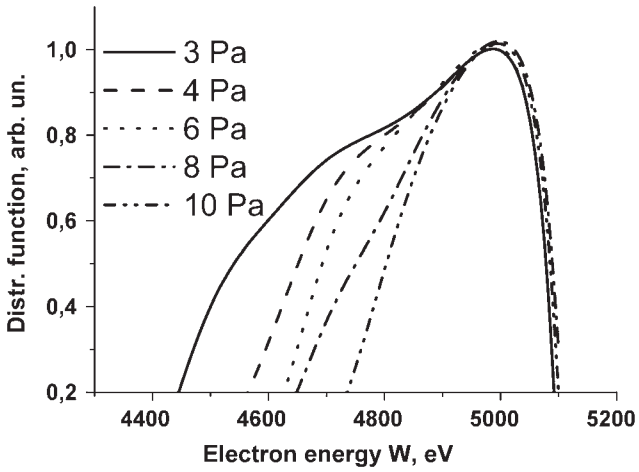

Fig. 12. Electron energy distribution in the beam for different pressures. The e-beam current was 36 mA and the accelerating voltage 5 kV.

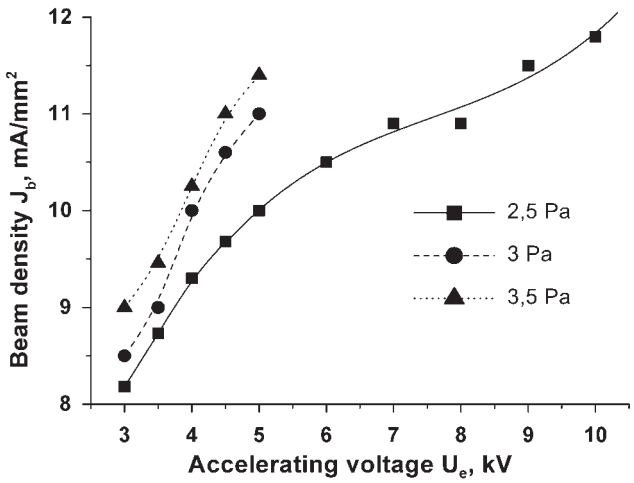

Fig. 14. E-beam current density J_b required for initiation of beam-plasma discharge *versus* accelerating voltage U_e, for different gas pressures.

initiation of the beam-plasma discharge increases with accelerating voltage and with gas pressure (Fig. 14).

The threshold current density j_e can be calculated using the criterion for initiation of a beam-plasma discharge in the form (Ivanov *et al.*, 1977)

$$\omega_{pe}\left(\frac{n_e}{n_i}\right)^{1/3} = 5\nu_{en}, \tag{8}$$

where ω_{pe} is the plasma frequency of electrons, n_e and n_i are the beam electron density and the plasma ion density, respectively, and ν_{en} is the electron-neutral collisions frequency. Simple transformations give

$$j_e = 25\sqrt{2}\nu_{en}^2\varepsilon_0\left(\frac{kT}{\pi M}\right)^{1/6}\left(\frac{m^2\lambda}{r_b e^2}\right)^{1/3} U_e^{1/3}, \tag{9}$$

where $(8kT/\pi M)^{1/2}$ is the thermal velocity of an ion, m, e are the electron mass and charge, r_b is the electron beam radius, and λ is the ionization mean free path for electrons. Eq. (9) adequately describes the mechanisms observed in the experiment. A more detailed description of e-beam transport for fore-vacuum plasma-cathode electron sources can be found in Zhirkov *et al.* (2006*a*).

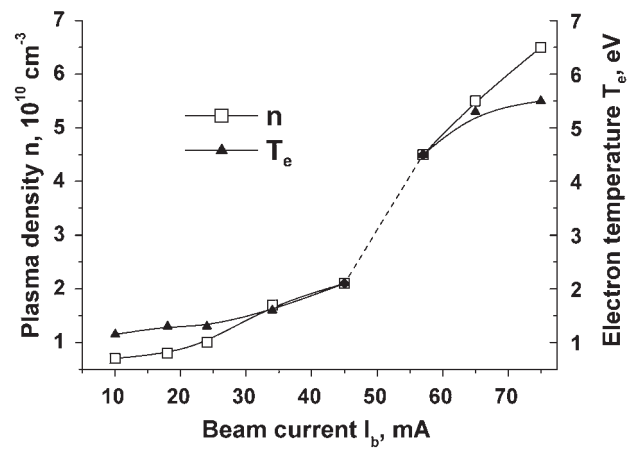

Fig. 13. Density n and temperature T_e of the beam plasma *versus* beam current. The pressure was 2.5 Pa and the accelerating voltage 5 kV.

3. DESIGN, PARAMETERS AND APPLICATIONS OF PLASMA ELECTRON SOURCES

Work on the generation of electron beams in the fore-pump pressure range by plasma-cathode electron sources have been reported elsewhere (Belyuk *et al.*, 1980). The success of these tests stimulated further detailed research on electron beam extraction from plasmas and on electron beam formation at (relatively) high background gas pressure. The total body of work has allowed the design of a number of versions of high-pressure plasma-cathode electron sources. The design and parameters of these sources, including beam configuration and dimensions, were dictated mainly by their specific required operating conditions and the function to be performed. In the following, we describe several fore-vacuum pressure plasma-cathode electron sources of focused and ribbon beams.

3.1. Plasma Source for Focused Electron Beams

A schematic of a fore-vacuum pressure plasma source for focused electron beams (Burdovitsin *et al.*, 2005) is shown in Figure 15, and a photograph in Figure 16. The source uses a traditional three-electrode system based on a hollow-cathode discharge. Hollow stainless steel cathode 1 of inner diameter 20 mm and height 60 mm is equipped with water jacket 2. The water jacket has two unions for water supply and removal. For increasing the plasma density, there is cathode insert 3 with 8 mm diameter hole on the system axis. The cathode insert is made of the same material

https://doi.org/10.1017/S0263034608000694 Published online by Cambridge University Press

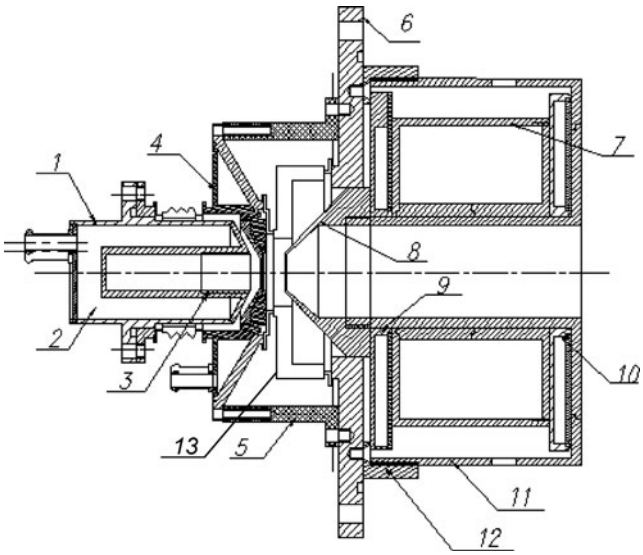

Fig. 15. Source schematic: cathode (**1**), water jacket (**2**), cathode insert (**3**), anode (**4**), dielectric supports (**5**), base flange (**6**), focusing coil frame (**7**), accelerating electrode (**8**), water jacket for cooling the focusing system (**9**, **10**), focusing system case (**11**), fastening of the focusing system (**12**), insulator of the acceleration gap (**13**).

as the hollow cathode. However, when a gas characterized by relatively high discharge operating voltage is used, e.g., argon, it is desirable to use an insert material of ion-electron yield greater than that of the cathode material, e.g., LaB_6, for example. This makes it possible to decrease the discharge voltage by 50–100 V. Anode 4 also has a water-cooling channel. Insulator 13 of the acceleration gap has a narrow section adjacent to the anode 4 for shielding its periphery and precluding high-voltage breakdown along so-called "long paths." The emission electrode is a stainless steel disk 1 mm thick with a 1 mm diameter central hole. Accelerating electrode 8 is placed on a threaded base flange. The current is increased using a tantalum plate with numerous emission holes of diameter 0.7–0.8 mm as the

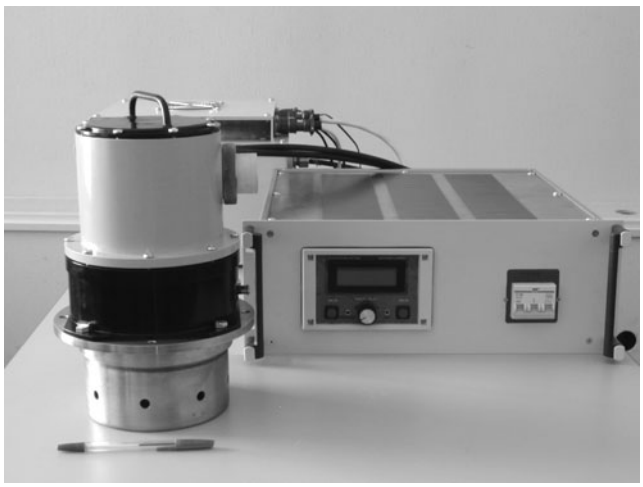

Fig. 16. Photograph of electron source with power supply equipment.

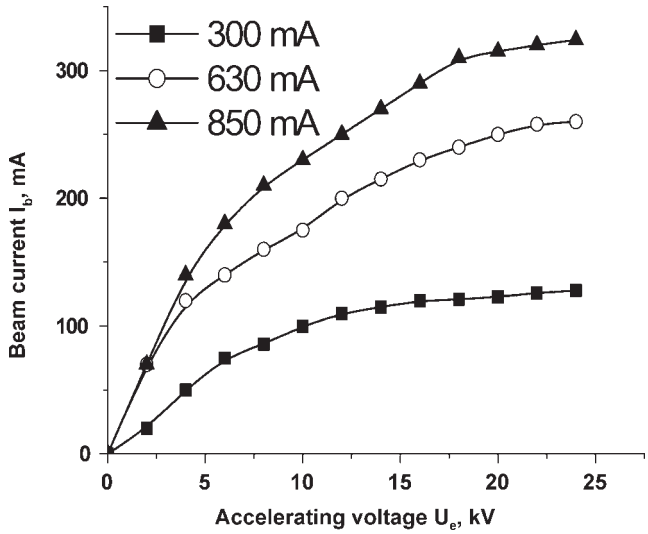

Fig. 17. Current-voltage characteristics for different discharge currents I_d. The emission electrode transparency was 40%.

emission electrode. A concave plate shape allows focusing the beam to a diameter of ~5 mm at a distance of ~30 cm from the beam extractor electrodes. The electrodes are water cooled in this design. To minimize current leakage, the cooling system is connected to the mains, using a high resistance water path. Magnetic lens 7 is used to focus the beam.

For this electron source, the beam current tends to saturate with increasing accelerating voltage (Fig. 17), whereas the emission characteristic is nearly linear (Fig. 18). This feature allows near-independent variation of beam current and electron energy. The source parameters are shown in Table 1.

The operating pressures for fore-vacuum electron sources (1–15 Pa) are greater than that employed for conventional plasma sources by about two orders. As indicated in the previous section, an important feature of e-beam generation

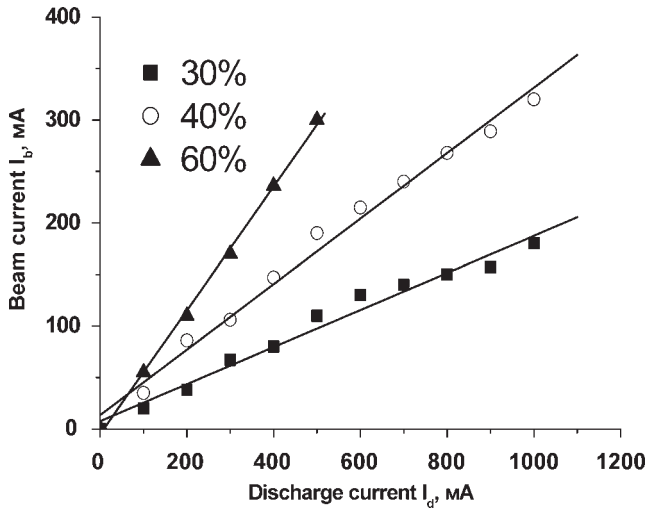

Fig. 18. E-beam current I_b *versus* discharge current I_d at $U_e = 15$ kV for different emission electrode transparency.

https://doi.org/10.1017/S0263034608000694 Published online by Cambridge University Press

Table 1. *Plasma electron source parameters*

Operating mode	Continuous
Discharge voltage	Up to 0.6 kV
Discharge current	Up to 1 A
Accelerating voltage	Up to 25 kV
Beam current	Up to 500 mA
Beam diameter (at up to 30 cm from the extractor)	3–5 mm
Electron beam power	Up to 7 kW
Working gas	Residual atmosphere, helium, air, methane, argon, etc.
Working gas pressure	1–15 Pa

at elevated pressures is the strong effect of back-streaming ions from the acceleration gap and beam transport region on the parameters of the electron source. In particular, these ions significantly affect the temperature of the electrode system of the plasma source, as evidenced by the dependence of the temperature T of the emission electrode on accelerating voltage U_e (Fig. 19). The influence of back-streaming ions on electrode heating has been confirmed by an experiment in which a ring electrode placed in the beam transport region scattered the back-streaming ion flux, a sizeable decrease in emission electrode temperature was observed. Note that thus judicious placement of a ring electrode can provide an efficient tool for decreasing the thermal load on the electrode system.

A more detailed description of the design features and parameters of fore-vacuum plasma sources for focused electron beams can be found elsewhere (Mytnikov *et al.*, 1998; Burdovitsin & Oks, 1999; Burdovitsin *et al.*, 2005; Burachevskii *et al.*, 2001).

3.2. Plasma Source for Ribbon Electron Beams

Interest in the generation of ribbon electron beams in the fore-vacuum pressure range is largely due to the possibility

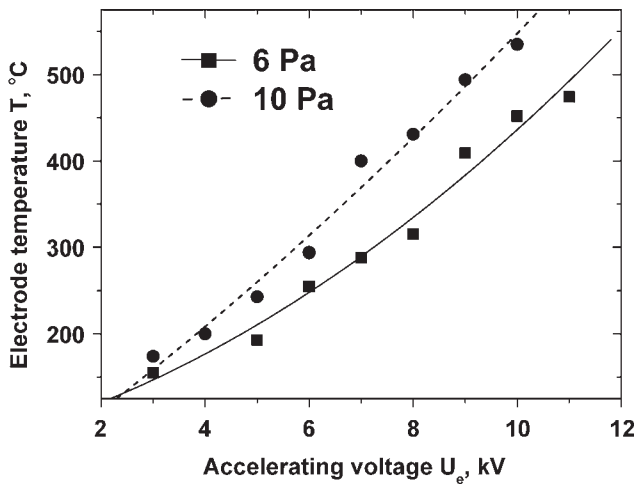

Fig. 19. Emission electrode temperature T *versus* accelerating voltage U_e for different pressures p. $I_d = 100$ mA.

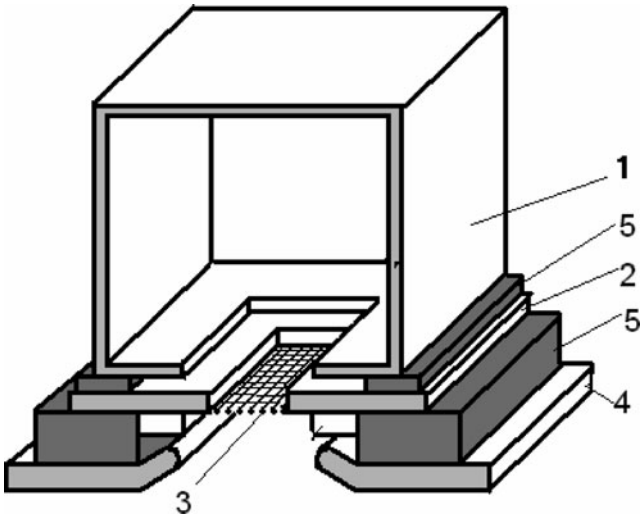

Fig. 20. Schematic of ribbon electron beam plasma source: hollow cathode (**1**), anode (**2**), emission grid (**3**), accelerating electrode (**4**), insulators (**5**).

of producing an extended plasma, a so-called plasma sheet (Burachevsky *et al.*, 2006) that can be used for ion-plasma treatment of large-cross-section flat surfaces. A schematic of a fore-vacuum pressure plasma-cathode ribbon electron beam source is shown in Figure 20, and a photograph in Figure 21 (Burdovitsin *et al.*, 2003*a*). The plasma chamber consists of water-cooled hollow cathode *1* of rectangular cross section and inner dimensions $300 \times 80 \times 40$ mm^3. In the cavity wall facing water-cooled anode 2, there is slot-hole of width 20 mm and length 280 mm parallel to a hole of dimensions 250×10 mm in the anode 2. The anode hole is covered with metal grid 3 with a 0.5×0.5 mm^2 mesh size. Accelerating electrode 4 is flat with a 300×20 mm^2 hole. The electrodes of the discharge and acceleration systems are separated by insulators *5* shielded from plasma and particle flow.

This source produces a ribbon electron beam of dimensions 250×10 mm^2, with energy 2–8 keV and current up to 500 mA at a gas pressure of 5–10 Pa. The operating mode is continuous. The emissivity, i.e., the ratio of the emission current to the discharge current, is >70%. The dependencies of the emission current I_e and the collector current I_b on accelerating voltage have distinct saturation regions (Fig. 22).

For ribbon electron beam sources, the beam current density distribution must usually be uniform only lengthwise. On the other hand, it is important to attain maximum current density. These requirements determine the geometry of the cross-sectionally non-uniform cathode cavity within the discharge chamber (Fig. 5b). As already noted, the narrow section of the cathode cavity provides increased plasma density near the emission boundary and hence increased electron beam current density due to the non-uniform plasma density distribution across the cavity, with a central maximum (Figs 7, 8). This maximum is due to plasma electron flow from the narrow section toward the

https://doi.org/10.1017/S0263034608000694 Published online by Cambridge University Press

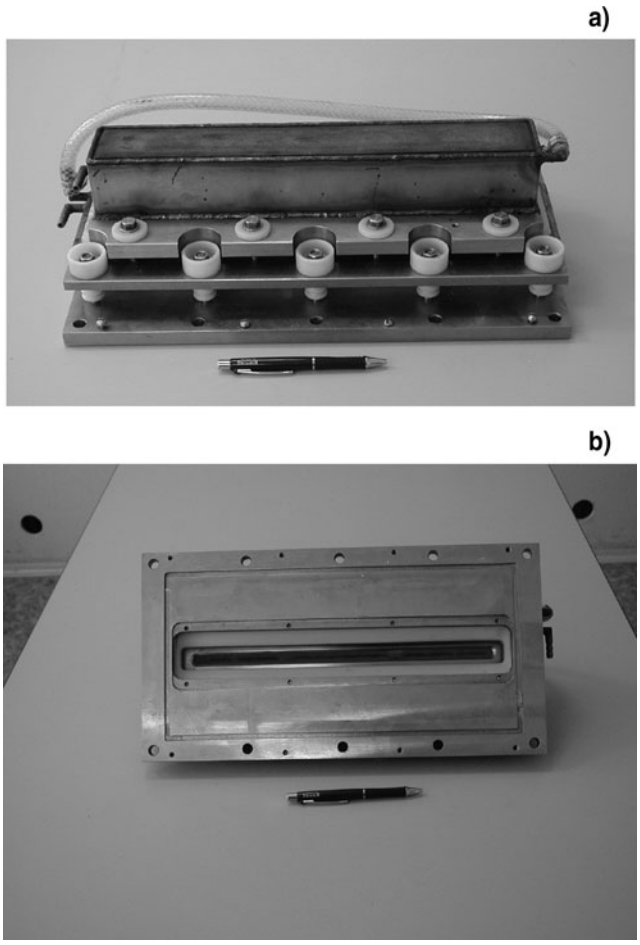

Fig. 21. Discharge chamber of ribbon electron beam plasma source from the side of the cathode (**a**) and emission hole (**b**).

slit-like emission aperture under the action of the electric field. A more detailed description of the design and parameters of this fore-vacuum ribbon electron beam source can be found in (Burdovitsin *et al.*, 2005).

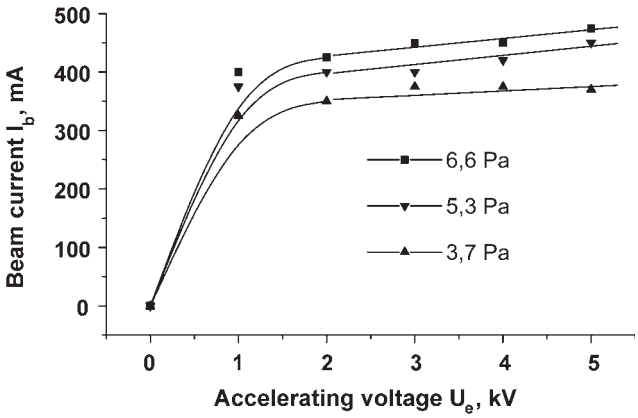

Fig. 22. Current-voltage characteristics of plasma electron source for discharge current $I_d = 500$ mA and different argon pressures.

3.3. Some Applications of Fore-Vacuum Pressure Electron Beams

3.3.1. Beam plasma generation

One promising application of electron beams is beam-assisted plasma generation. The method can be used for the formation of highly uniform plasma of large volume. Such plasma may differ significantly from plasmas produced in more usual electrode and electrode less discharges. Since the gas is ionized without electric field, the differences concern primarily the electron temperature T_e, which may range from fractions of an electron volt (Leonhardt *et al.*, 2007) up to $\sim$100 eV (Ivanov, 1999) depending on the details of the beam-plasma interaction. Collisional interactions are characterized by small values of T_e, whereas collective interactions result in a beam-plasma discharge with high values of T_e (Ivanov & Leiman, 1977). A beam-plasma discharge is distinguished by high energy efficiency, since beam electrons interacting collectively with plasma electrons transfer most of the beam energy to the plasma. Which kind of interaction dominates depends on the interaction conditions. For low beam current density, collisional interactions always dominate, whereas for high current density and appropriate gas pressure, the prevailing interaction mechanism is collective. The choice of the mode is dictated by the task for which the plasma is produced.

In the experiments described below, a ribbon electron beam was formed using the source described in the previous section. The experimental arrangement is shown in Figure 23 (Burdovitsin *et al.*, 2004*a*). Electron beam **1** formed by plasma source **2** has a cross section of 250×10 mm^2 at the exit of the emission hole. A magnetic field parallel to the beam propagation direction is used to minimize beam spread and confine the plasma. Two coils of rectangular cross-section produce the magnetic field.

The working gas (argon) is supplied directly to the working chamber. The distribution of the e-beam current density over the beam cross section was investigated using collector **3** movable along two coordinates with a collimating aperture of diameter 3 mm. The plasma parameters were

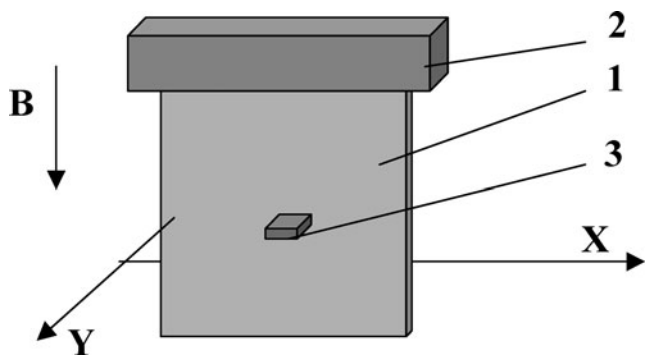

Fig. 23. Schematic of plasma sheet formation: electron beam (**1**), electron source (**2**), collector (**3**).

https://doi.org/10.1017/S0263034608000694 Published online by Cambridge University Press

measured using a double probe arranged inside the collector in such a way that the beam did not directly see the probes. The probes were made of a 1 mm diameter tungsten wire inside a ceramic tube and protruding by 2 mm.

Figure 24 shows typical distributions of the beam current density, electron temperature and plasma density in the plane perpendicular to the beam propagation (Burdovitsin *et al.*, 2004*b*). The electron temperature depends little on the spatial coordinate and lies in the range 2 to 4 eV. The dependencies indicate reasonable uniformity of the beam and plasma density distributions along the X axis (Figs 24b, 24c). This suggests that this electron source can be used for producing large area plasmas and allows us to estimate the contributions of various processes to plasma formation. Figure 25 shows the measured dependencies of plasma density on the coordinate Y in the middle part of the plasma sheet (along the axis X). The parameters are total beam current, gas pressure, and magnetic field. The figure demonstrates that increasing the gas pressure increases the plasma density. A similar increase in plasma density is observed with increasing beam current. As the strength of the longitudinal magnetic field is increased, the plasma density distribution starts to "sharpen" (Fig. 25b).

The experimental dependencies suggest that the spatial distribution of the plasma parameters is governed in the main by the beam electron current density distribution. At the same time, comparison of Figures 25a and 25b indicates that diffusion processes contribute significantly to the "smoothing" of the plasma density distribution. A proposed model (Burdovitsin *et al.*, 2004*b*) describes the processes rather well, as evidenced by good agreement between the calculations and experimental data. However, the model predicts a stronger magnetic field effect on the distribution than observed experimentally. We think that this implies the need to take into account particle motion not only crosswise, but also lengthwise with respect to the magnetic field.

The research results suggest that the ribbon electron beam produced by the fore-vacuum pressure plasma-cathode e-beam source can be used to advantage to form a large-area, uniform plasma sheet. The plasma density obtained in the experiment suffices for efficient film deposition and surface modification of large-area flat materials.

The plasma produced by a ribbon beam in hydrocarbon gases (e.g., propane, butane) has been used for deposition of hard carbon coatings (Burdovitsin *et al.*, 2003*b*). The deposition rate was determined by the beam current and was nonmonotonically dependent on the beam−substrate spacing (Fig. 26). A decrease in deposition rate for small distances stems from sputtering of the coating by ions accelerated by the potential difference between plasma and substrate. X-ray photoelectron spectroscopy (XPS) spectra indicate that the deposited coatings contain up to 90% carbon, have a polymer-like structure, and, without taking special measures, display a hardness of 1–1.5 GPa. Radio frequency (RF) bias applied to the substrate leads to further increase of the coating hardness by up to an order of magnitude.

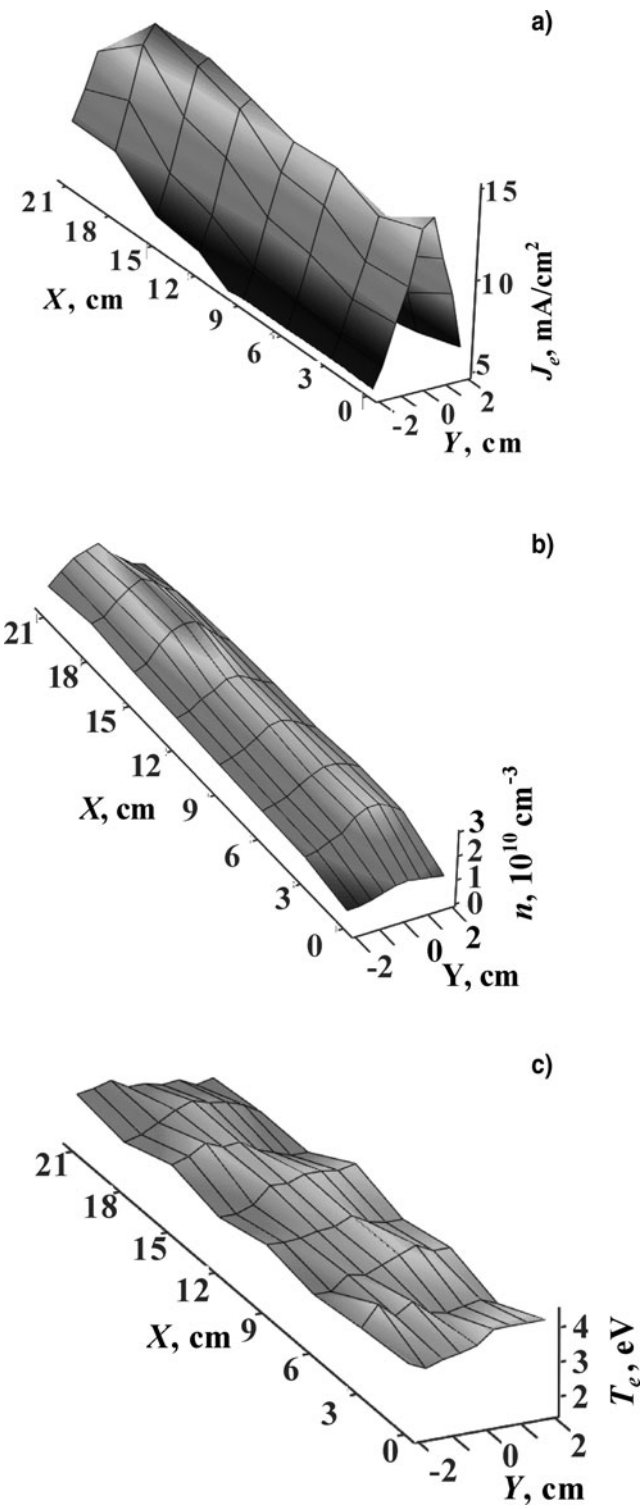

Fig. 24. Distribution of beam density (**a**), plasma density (**b**), and plasma electron temperature (**c**) in the plane perpendicular to beam propagation.

3.3.2. Metal evaporation and coating synthesis

Electron-beam evaporation of metals is now a widely used technological process. In this process, the electron beam is typically generated using hot-cathode electron gun, and this imposes limits on the presence of active gases, particularly

https://doi.org/10.1017/S0263034608000694 Published online by Cambridge University Press

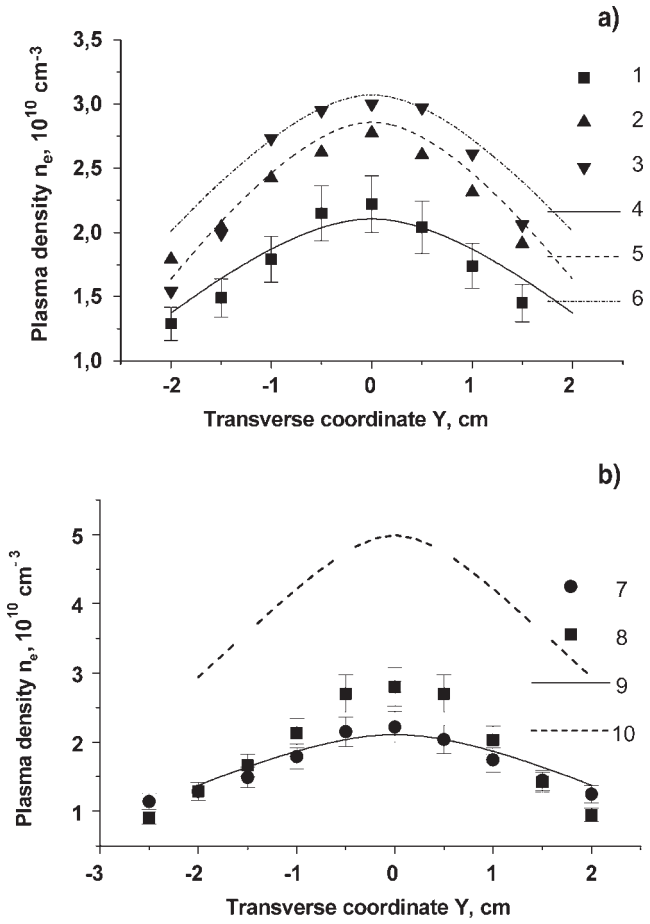

Fig. 25. Experimental (1–3, 7, 8) and calculated (4–6, 9, 10) plasma density distributions for different emission currents I_e and Ar pressures p (**a**) and magnetic fields B (**b**): $I_e = 400$ mA (1, 2, 4, 5, 7–10), 600 mA (3, 6), $p = 6$ Pa (1, 3, 4, 6–10), 9 Pa (2, 5), $B = 5.4$ mT (1–7, 9), 10.5 mT (8, 10).

oxygen, in the working volume. Although the electron beam ionizes the metal vapor, associated plasma research has been limited. A possible reason for this may be that the ion component counts little in the coating deposition. There can be a

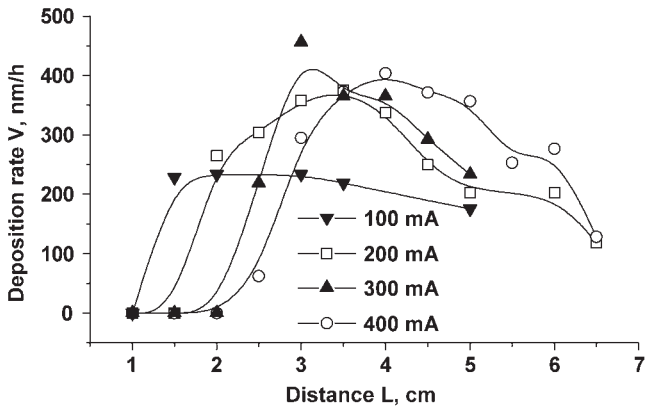

Fig. 26. Carbon films deposition rate V as a function of beam–substrate distance L for different beam currents.

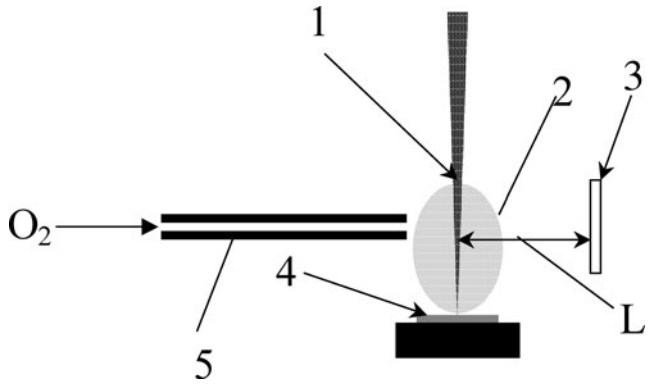

Fig. 27. Experimental arrangement for deposition of oxide coatings: electron beam (**1**), expected region of metal plasma formation (**2**), substrate (**3**), target (**4**), oxygen supply tube (**5**).

radical change in the situation if metal evaporation and hence coating deposition is carried out using reactive gases, e.g., oxygen. In this case, the composition and properties of the deposited films may depend strongly on the metal ion plasma. Electron-beam evaporation of materials allows the film parameters to be varied over a wide range.

Figure 27 shows a schematic of the experimental arrangement used for electron-beam evaporation in the fore-vacuum pressure range. Target 4 was made either of titanium or copper. Tube 5 is used to supply oxygen to the region where metal plasma 2 is expected to develop. The coatings were deposited on silicon substrate 3 located at a distance L from the beam axis. The curves in Figure 28 demonstrate the correlation between the density of the generated metal plasma and the deposited beam power. The deposition rate depends on the substrate—beam axis spacing and is about 1–1.5 μm/min.

A more detailed description of the use of fore-vacuum plasma sources for this application can be found in

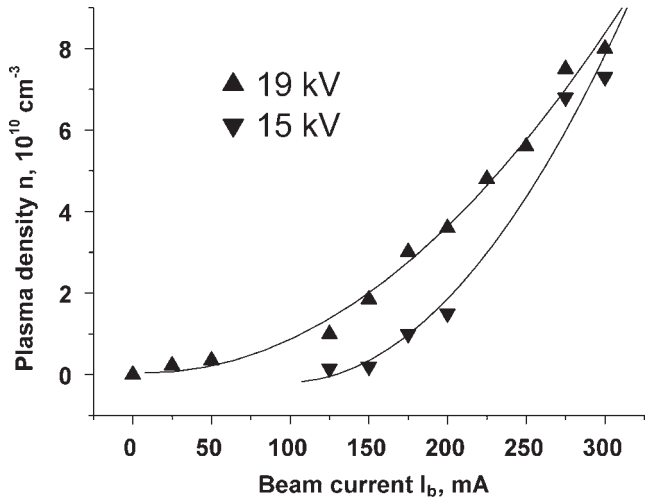

Fig. 28. Metal plasma density n *versus* beam current I_b for a Cu target at different accelerating voltages. The pressure was 9 Pa.

https://doi.org/10.1017/S0263034608000694 Published online by Cambridge University Press

Burachevsky (2003). Special experiments were carried out on carbon nanostructures preparation by graphite target electron beam evaporation (Medovnik, 2008).

4. CONCLUSION

The fundamental advantage of plasma-cathode electron sources is their capability of beam production at elevated pressures of up to fore-vacuum pressures. The operation of these devices at relatively high pressures has some unique features, including the large effect of back-streaming ion flow from the acceleration gap and beam transport region on the discharge operation and on the plasma emissivity. Moreover, the positive feedback between the ion current and the electron emission current can lead to instability of the plasma emission boundary and subsequent breakdown of the acceleration gap. In the case of large-cross-section electron beams generated in the fore-vacuum pressure range, the back-streaming ion flow greatly increases the non-uniformity of the beam current density distribution. Thus formation of an initially uniform plasma emission surface is critical for these high pressure electron sources. Another important concern is to provide sufficient electric field strength in the acceleration gap with due regard to high voltage breakdown at the periphery along "long paths".

Despite some difficulties in operation of these kinds of sources in the fore-vacuum pressure range, research in the field has made it possible to design radically new e-beam sources that provide continuous production of focused and ribbon electron beams with parameters attractive for their efficient application in electron-beam technologies such as metal surface modification, plasma chemistry, and more.

ACKNOWLEDGEMENTS

The authors are grateful to colleagues and postgraduates in the Plasma Electronics Laboratory of the Physics Department at Tomsk State University of Control Systems and Radioelectronics for their contributions to the development and improvement of fore-vacuum pressure plasma-cathode electron sources. Special thanks to Dr. Ian Brown (Berkeley Lab) for useful discussions and improvement of English. Russian Foundation for Basic Research grant RFBR No. 08-08-00015 is gratefully acknowledged.

REFERENCES

Belyuk, S.I., Kreindel, Yu.E. & Rempe, N.G. (1980). Research of possibility of expansion of area of pressure of a plasma source электронов. *Soviet Phys. Techn. Phys.* **25**, 124.

Bugaev, S.P., Kreindel, Yu.E. & Schanin, P.M. (1984). *Large-Cross-Section Electron Beam* (in Russian). Moscow: Energoatomizdat.

Bugaev, A.S., Vizir, A.V., Gushenets, V.I., Nikolaev, A.G., Oks, E.M., Yushkov, G.Yu., Burachevsky, Yu.A., Burdovitsin, V.A., Osipov, I.V. & Rempe, N.G. (2003). Current status of the plasma emission electronics. *Laser Part. Beams* **21**, 139.

Burachevskii, Y.A., Burdovitsin, V.A., Kuzemchenko, M.N., Mytniko, V.A.V. & Oks, E.M. (2001). Generation of electron beams in fore-vacuum pressure range. *Russian Phys. J.* **44**, 996.

Burachevsky, Yu.A., Burdovitsin, V.A., Mytnikov, A.V. & Oks, E.M. (2001). Limiting working pressure of a plasma electron source on the basis of hollow cathode discharge. *Techn. Phys.* **46**, 179.

Burachevsky, Y.A., Burdovitsin, V., Oks, E. & Fedorov, M. (2003). Film synthesis in a beam-plasma discharge driven by electron beam from the fore-pump plasma gun. *Proc. 7th Int. Conf. on Electron Beam Technologies*, p. 160. Bulgaria.

Burachevsky, Yu.A., Burdovitsin, V.A., Oks, E.M., Klimov, A.S. & Fedorov, M.V. (2006). Plasma localization in an extended hollow cathode of the plasma source of a ribbon electron beam. *Techn. Phys*. **51**, 1316.

Burdovitsin, V.A. & Oks, E.M. (1999). Hollow-cathode plasma electron gun for beam generation at fore-pump gas pressure. *Rev. Sci. Instrum*. **70**, 2975.

Burdovitsin, V.A., Kuzemchenko, M.N. & Oks, E.M. (2002). Electric strength of an accelerating gap of plasma electron source in fore-vacuum pressure range. *Techn. Phys*. **47**, 926.

Burdovitsin, V.A., Burachevskii, Yu.A., Oks, E.M. & Fedorov, M.V. (2003*a*). A Plasma-cathode electron source for ribbon-beam generation at fore-vacuum pressures. *Instr. Exper. Techn*. **46**, 257.

Burdovitsin, V., Burachevsky, Yu., Oks, E. & Rabotkin, S. (2003*b*). Initiation of plasma chemistry reaction with electron beam, produced by plasma electron gun. *Proc. 16th Int. Symp. On Plasma Chemistry*, Italy.

Burdovitsin, V.A., Burachevsky, Yu.A., Oks, E.M. & Fedorov, M.V. (2004*a*). Specific features of the formation of a uniform ribbon electron beam by a plasma source in the fore-vacuum pressure range. *Techn. Phys*. **49**, 104.

Burdovitsin, V.A., Oks, E.M. & Fedorov, M.V. (2004*b*). Parameters of the plasma sheet generated by ribbon electronic beam in fore-vacuum pressure range. *Russian Phys. J*. **47**, 310.

Burdovitsin, V.A., Zhirkov, I.S., Oks, E.M. & Osipov, I.V. (2005). A plasma-cathode electron source for focused-beam generation in the fore-pump pressure range. *Instr. Exper. Techn*. **48**, 761.

Denbnovetsky, S.V., Melnyk, V.G. & Melnyk, I.V. (2003). High voltage glow discharge electron sources and possibilities of its technological application. *IEEE Trans. Plasma. Sci*. **31**, 987.

Dewald, E., Frank, K., Hoffmann, D.H.H., Ganciu, M., Mandache, N.B., Nistor, M., Pointu, A.M. & Popescu, I.I. (1998). Intense electron beams produced in pseudospark and PCOHC for beam-plasma interaction experiments. *Nucl. Instr. Meth. Phys. Res. A* **415**, 614–620.

Frank, K., Bickes, C., Ernst, U., Iberler, M., Meier, J., Prucker, U., Schlaug, M., Schwab, J., Urban, J. & Hoffmann, D.H.H. (1998). Low-pressure pseudospark switches for ICF pulsed power. *Nucl. Instr. Meth. Phys. Res. A* **415**, 327–331.

Frank, K., Dewald, E., Bickes, C., Ernst, U., Iberler, M., Meier, J., Prucker, U., Rainer, A., Schlaug, M., Schwab, J., Urban, J., Weisser, W. & Hoffmann, D.H.H. (1999). Scientific and technological progress of pseudospark devices. *IEEE Trans. Plasma Sci*. **27**, 1008–1020.

Galansky, V.L., Kreindel, Yu.E., Oks, E.M. & Ripp, A.G. (1987). Analysis of the emission properties of a plasma cathode. *Soviet Phys. Techn. Phys*. **32**, 905.

Goebel, D.M. & Watkings, R.M. (2000). High current low pressure plasma cathode electron gun. *Rev. Sci. Instrum*. **71**, 388.

Gruzdev, V.A., Kreindel, Yu.E. & Larin, Yu.M. (1974). Effect of ionization on the position of the emitting surface of the plasma in a high-voltage gap with a plasma cathode. *Soviet Phys. Techn. Phys*. **18**, 1465.

Gushenets, V.I., Oks, E.M., Yushkov, G.Yu. & Rempe, N.G. (2003). Current status of the plasma emission electronics. I. Basic physical processes. *Laser Part. Beams* **21**, 123.

Hershcovitch, A. (1993). Observation of a very high electron current extraction mode in a hollow cathode discharge. *J. Appl. Phys*. **74**, 728.

Ivanov, A.A. & Leiman, V.G. (1977). Ignition of a beam-plasma discharge by an intense electron beam. *Plasma Phys. Rept*. **3**, 780.

Ivanov, A.A., Serov, A.A., Kniazev, L.N. & Muraviov, S.V. (1999). Efficiency of Electron-beam energy deposition in a beam-plasma discharge. *Plasma Phys Rept*. **25**, 46–52.

Klimov, A.S., Burdovitsin, V.A. & Oks, E.M. (2007). Plasma localization in extended hollow cathode of ribbon electron beam plasma source in fore-vacuum pressure range. *Russian Phys. J*. **50**, 310.

Klimov, A.S., Burdovitsin, V.A., Burachevsky, Yu.A. & Oks, E.M. (2008). Inhomogeneous extended hollow cathode discharge for raising the current density in a fore-vacuum plasma source of a ribbon electron beam. *Techn. Phys*. **53**, 432–435.

Koval, N.N., Oks, E.M., Kreindel, Yu.E., Schanin, P.M. & Gavrilov, N.V. (1992). Broad beam electron guns with plasma cathodes. *Nucl. Instr. Meth. Phys. Res. A* **312**, 417.

Koyama, K., Adachi, M., Miura, E., Kato, S., Masuda, S., Watanabe, T., Ogata, A. & Tanimoto, M. (2006). Monoenergetic electron beam generation from a laser-plasma accelerator. *Laser Part. Beams* **24**, 95–100.

Krasik, Ya.E., Gleizer, J.Z., Krokhmal, A., Chirko, K., Sayapin, A., Felsteiner, J., Bernshtam, V. & Gushenets, V.I. (2005). High-current electron sources based on gaseous discharges. *Vacuum* **77**, 391.

Kreindel, Yu.E. (1977). *Plasma Electron Sources* (in Russian). Moscow: Atomizdat.

Leonhardt, D., Walton, S.G. & Fernsler, R.F. (2007). Fundamentals and applications of a plasma-processing system based on electron-beam ionization. *Phys. Plasmas*. **14**, 057103.

Lifschitz, A.F., Faure, J., Glinec, Y., Malka, V. & Mora, P. (2006). Proposed scheme for compact GeV laser plasma accelerator. *Laser Part. Beams* **24**, 255–259.

Liu, J.L., Yin, Y., Ge, B., Zhan, T.W., Chen, X.B., Feng, J.H., Shu, T., Zhang, J.D. & Wang, X.X. (2007). An electron-beam accelerator based on spiral water PFL. *Laser Part. Beams* **25**, 593–599.

Liu, J.L., Zhan, T.W., Zhang, J., Liu, Z.X., Feng, J.H., Shu, T., Zhang, J.D. & Wang, X.X. (2007). A Tesla pulse transformer for spiral water pulse forming line charging. *Laser Part. Beams* **25**, 305–312.

Mangles, S.P.D., Walton, B.R., Najmudin, Z., Dangor, A.E., Krushelnick, K., Malka, V., Manclossi, M., Lopes, N., Carias, C., Mendes, G. & Dorchies, F. (2006). Table-top laser-plasma acceleration as an electron radiography source. *Laser Part. Beams* **24**, 185–190.

Medovnik, A.V., Burachevsky, Yu.A., Burdovitsin, V.A. & Oks, E.M. (2008). Carbon films, prepared by electron beam evaporation of graphite target. *Proc. of 9th Int. Conf. on Modification of Materials with Particle Beams and Plasma Flows*, Tomsk, Russia.

Mytnikov, A.V., Oks, E.M. & Chagin, A.A. (1998). The plasma cathode electron source for generation of beams in fore-vacuum pressure range. *Instr. Exper. Techn*. **41**, 234.

Nakamura, T., Sakagami, H., Johzaki, T., Nagatomo, H. & Mima, K. (2006). Generation and transport of fast electrons inside cone targets irradiated by intense laser pulses. *Laser Part. Beams* **24**, 5–8.

Niu, H.Y., He, X.T., Qiao, B. & Zhou, C.T. (2008). Resonant acceleration of electrons by intense circularly polarized Gaussian laser pulses. *Laser Part. Beams* **26**, 51–59.

Oks, E.M. (1992). Physics and technique of plasma electron sources. *Plasma Sour. Sci. Technol*. **1**, 249.

Oks, E.M. & Schanin, P.M. (1999). Development of plasma cathode electron guns. *Phys. Plasmas* **7**, 1649.

Oks, E.M. (2006). *Plasma Cathode Electron Sources – Physics, Technology, Applications*. Weinheim, Germany: Wiley-VCH.

Osipov, I.V. & Rempe, N.G. (2000). A plasma-cathode electron source designed for Industrial use. Review of scientific instruments. *Rev. Sci. Instrum*. **71**, 1638.

Raizer, Y.P. (1991). *Gas Discharge Physics*. Berlin: Springer-Verlag.

Sakai, K., Miyazaki, S., Kawata, S., Hasumi, S. & Kikuchi, T. (2006). High-energy-density attosecond electron beam production by intense short-pulse laser with a plasma separator. *Laser Part. Beams* **24**, 321–327.

Vizir, A.V., Oks, E.M., Schanin, P.M. & Yushkov, G.Yu. (1997). Non-sustainable glow hollow cathode discharge for wide-aperture ionic sources. *Techn. Phys*. **42**, 611.

Wong, C.S., Woo, H.J. & Yap, S.L. (2007). A low energy tunable pulsed X-ray source based on the pseudospark electron beam. *Laser Part. Beams* **25**, 497–502.

Zaviyalov, M.A., Kreindel, Yu.E., Novikov, A.A. & Shunturin, L.P. (1989). *Plasma processes in Technological Electron Guns* (in Russian). Moscow: Energoatomizdat.

Zharinov, A.V., Kovalenko, Yu.A., Roganov, I.S. & Teryukanov, P.M. (1986*a*). The plasma electron emitter with grid stabilization. *Soviet Phys. Techn. Phys*. **31**, 39.

Zharinov, A.V., Kovalenko, Yu.A., Roganov, I.S. & Teryukanov, P.M. (1986*b*). Theory of electron collectors in gas discharge. *Soviet Phys. Techn. Phys*. **31**, 413.

Zhirkov, I.S., Burdovitsin, V.A., Oks, E.M. & Osipov, I.V. (2006*a*). Formation of narrow-focused electron beams generated by a source with a plasma cathode in the fore-vacuum pressure range. *Techn. Phys*. **51**, 786.

Zhirkov, I.S., Burdovitsin, V.A., Oks, E.M. & Osipov, I.V. (2006*b*). Discharge initiation in a hollow-cathode plasma source of electrons. *Techn. Phys*. **51**, 1379.

Zhirkov, I.S., Burdovitsin, V.A. & Oks, E.M. (2007). Influence of the longitudinal magnetic field in the accelerating gap on the limiting parameters of a plasma electron source operating in the fore-vacuum pressure range. *Techn. Phys*. **52**, 1217.